Pergamon

Journal of Structural Geology, Vol. 18, No. 1, pp. 41 to 59, 1996

0191–8141/96 $15.00+0.00

0191–8141(95)00075–5

Crustal-scale strain partitioning: footwall deformation below the Alpine Oligo-Miocene detachment of Corsica

JEAN-MARC DANIEL, LAURENT JOLIVET,* BRUNO GOFFE and CHRISTOPHE POINSSOT

Département de Géologie, Ecole Normale Supérieure, 24 rue Lhomond, 75232 Paris Cedex 05, France

(*Received* 21 *April* 1994; *accepted in revised form* 26 *June* 1995)

Abstract—The Alpine metamorphic units of Corsica were exhumed in the footwall of an Oligo-Miocene detachment. New structural data are used to describe the ductile deformation within the footwall and its evolution from greenschist facies metamorphic conditions to the surface. Regional variations in the type of kinematic indicators show a partitioning between vertical coaxial shortening and localized non-coaxial flow on extensional ductile shear zones. Coaxial flow results in folding with axial-plane crenulation cleavage that is horizontal or gently W dipping. Slightly curved fold axes and a general asymmetry indicate a minor component of eastward shear. Non-coaxial flow results in the formation of a mylonitic foliation dipping to the E associated with top-to-the-east sense of shear. This distribution is seen at all scales from the thin section to that of the crust. At crustal-scale, vertical coaxial shortening occurs within large boudins bounded by plurikilometric extensional shear zones. As exhumation proceeded, the footwall entered the brittle field. Late deformation is then characterized by subvertical shear and large scale folding, interpreted in terms of isostatic re-equilibration during denudation. Tectonic activity ends with normal faulting and deposition of marine sediments in asymmetric grabens. This description illustrates the behaviour of the ductile crust beneath upper crustal tilted blocks.

INTRODUCTION

During the past decade, studies dealing with metamorphic core complexes have mostly focused on precise descriptions of detachment faults and only a few papers have described internal deformation of the footwall. However, several lines of reasoning show that a large amount of strain has to be distributed in the footwall of major detachments. For example, Block & Royden (1990) and Wdowinsky & Axen (1992) have shown that when the crust is unloaded by the activity of a detachment fault, it yields in a viscous manner that can explain some major features observed in metamorphic core complexes: doming of foliation, late layer parallel contraction and subvertical shear (Wernicke & Axen 1988, Bartley & Fletcher 1990). These features are known to develop in the latest history of metamorphic core complexes. Earlier ductile deformation often predates these events. For example, Miller *et al.* (1983) described pervasive vertical coaxial shortening as an early result of extension, before the inception of localized simple shear. In addition, Bird (1991) demonstrated that the lower crust can flow when a topographic high exists.

Alpine Corsica was isolated from the Alps when lithospheric stretching started in the Early Oligocene in the Liguro–Provençal Basin and then in the Middle Miocene in the Tyrrhenian Sea (Fig. 1) (Burrus 1984, Réhault *et al.* 1984, Sartori *et al.*, 1987, Dewey *et al.* 1989). Jolivet *et al.* (1990) and Fournier *et al.* (1991) have shown that Alpine Corsica can be considered as a metamorphic core complex of Oligo-Miocene age similar to the Basin and Range and Aegean Sea. Below a sharp detachment between metamorphic and non-metamorphic units, deformation of the footwall results in both pervasive flattening and localized simple shear at all scales.

GEOLOGICAL SETTING

Main units

Alpine Corsica is a nappe stack formed in the Late Cretaceous and Eocene by underthrusting of the continental margin of Europe made of Hercynian plutonic rocks, under Ligurian oceanic units (Caron 1977, Caron *et al.* 1981, Mattauer *et al.* 1981, Amaudric du Chaffaut 1982, Durand Delga 1984). The nappe stack can be described as follows (Figs. 2 and 3), from base to top:

External units. The Tenda Massif mainly consists of granitic rocks belonging to the European margin. It has been deformed and metamorphosed during Late Cretaceous/Eocene thrusting of the Schistes Lustrés Nappe toward the west (Mattauer *et al.* 1981, Gibbons & Horak 1984, Warburton 1986, Jourdan 1988). It is thought to be either the autochthonous basement (Mattauer *et al.* 1981, Gibbons & Horak 1984, Waters 1990) or a thrust sheet slightly displaced toward the west during shortening of the European margin (Warburton 1986, Jourdan 1988).

To the south, the Corte Units are imbricated in a nappe stack which involves basement and its sedimen-

*Present address: Département des Sciences de la Terre, Université de Cergy-Pontoise, Avenue du Parc, 8 le Campus, 95033 Cergy-Pontoise Cedex, France.

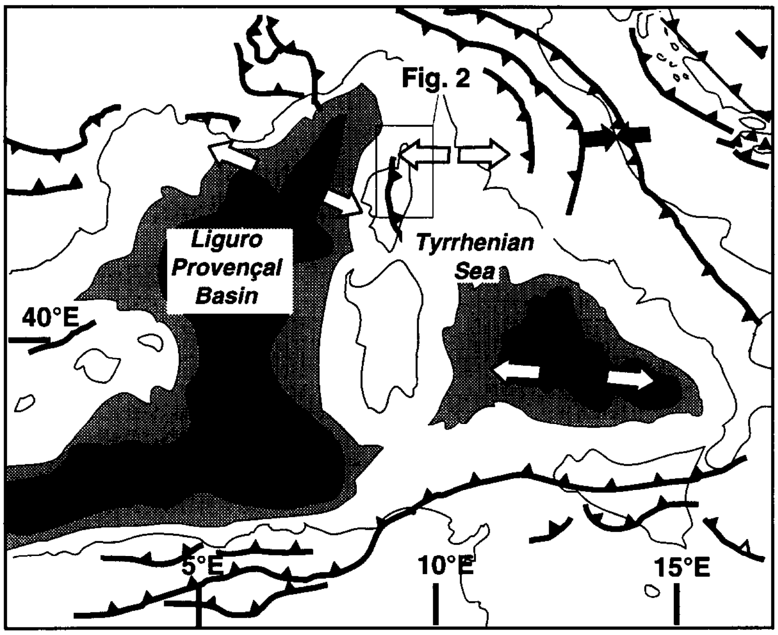

Fig. 1. Location map of Corsica between the Liguro–Provençal Basin and the Tyrrhenian Sea. Lighter shading shows highly thinned continental crust and darker shading shows oceanic crust. Double arrows show the approximate direction of Cenozoic extension or compression.

tary cover (Amaudric du Chaffaut 1982, Bézert & Caby 1989, Egal 1992), along the contact between Alpine Corsica and autochthonous Western Corsica. The latter is mainly made of Hercynian rocks, locally overlain by Eocene sediments.

The Schistes Lustrés Nappe sensu lato. This rests upon the Tenda Massif by a shear zone initially formed in high *P*–low *T* conditions, with top-to-the-west sense of shear (Mattauer *et al.* 1981), later reworked as a ductile normal fault during retrogression in the greenschist facies (Waters 1989, Jolivet *et al.* 1991). This nappe comprises several oceanic and continental units. Oceanic units are similar to the Schistes Lustrés Nappe of the Western Alps (Caron 1977) in terms of lithofacies and metamorphic grade. In the south of Alpine Corsica, the Schistes Lustrés Nappe is in contact with either the Corte Units, or the Hercynian basement and its Eocene cover.

The upper unit (called hereafter the Balagne Nappe). This is characterized by a lack of metamorphism and ductile deformation. It is constituted chiefly of ophiolitic material and oceanic sediments of Late Jurassic age as well as Late Cretaceous flysch (Durand Delga 1984). It rests upon all metamorphic units by a sharp contact subsequently folded into broad antiforms and synforms. It is distributed in three areas: (1) the Balagne Nappe *sensu stricto* rests upon non-metamorphosed Eocene autochthonous sediments west of the Tenda Massif; (2) the Nebbio Klippe; and (3) the Macinaggio Klippes in the Centuri region rest upon the Schistes Lustrés Nappe. This superficial nappe was emplaced in the Middle Eocene above Western Corsica, as attested by the presence of olistostrome deposits in the autochthonous Eocene Basin below the Balagne Nappe *sensu stricto* (Durand Delga 1984, Jourdan 1988). Beneath the Nebbio Klippe, poorly metamorphosed acidic rocks crop out within the contact zone. They are similar to various facies of the Tenda Massif, though less deformed.

All these units are unconformably overlained by terrestrial to shallow marine deposits of Early Miocene age (Francardo and St Florent Basins).

Geological evolution

There is a general agreement about the early history of Alpine Corsica. The first stage is represented by the occurrence, in several units, of eclogitic associations indicating a minimum pressure of 11 kb for temperatures about 400°C (Caron *et al.* 1981, Harris 1984, Lahondère 1988, Fournier *et al.* 1991). These associations were retrogressed in the blueschist facies, during the Late Cretaceous and Eocene. Blueschist facies parageneses are widespread in Alpine Corsica and correspond to pressure and temperature in the range of 6–7 kb and 330–400°C (Harris 1984, Gibbons *et al.* 1986, Lahondère 1988, Waters 1989). Occurrence of jadeite and almost pure glaucophane argue for even higher pressure, up to 10 kb in the same temperature range (Peterlongo 1968, Essene 1969, Ohnenstetter *et al.* 1976, Evans 1990). Related deformation, referred as D_1 in the literature (Gibbons *et al.* 1986 for a review), leads to the formation of the Schistes Lustrés Nappe which was emplaced on the Hercynian basement of Western Corsica (Gibbons & Horak 1984) and its Eocene cover (Egal & Caron 1988, Egal 1992). D_1 is characterized by the development of strong LS fabrics (with L_1 striking approximately east–west at the latitude of Bastia) and top-to-the-west sense of shear (Faure & Malavieille 1981, Mattauer *et al.* 1981). D_1 ended in the Late Eocene (Egal & Caron 1988, Bézert & Caby 1989).

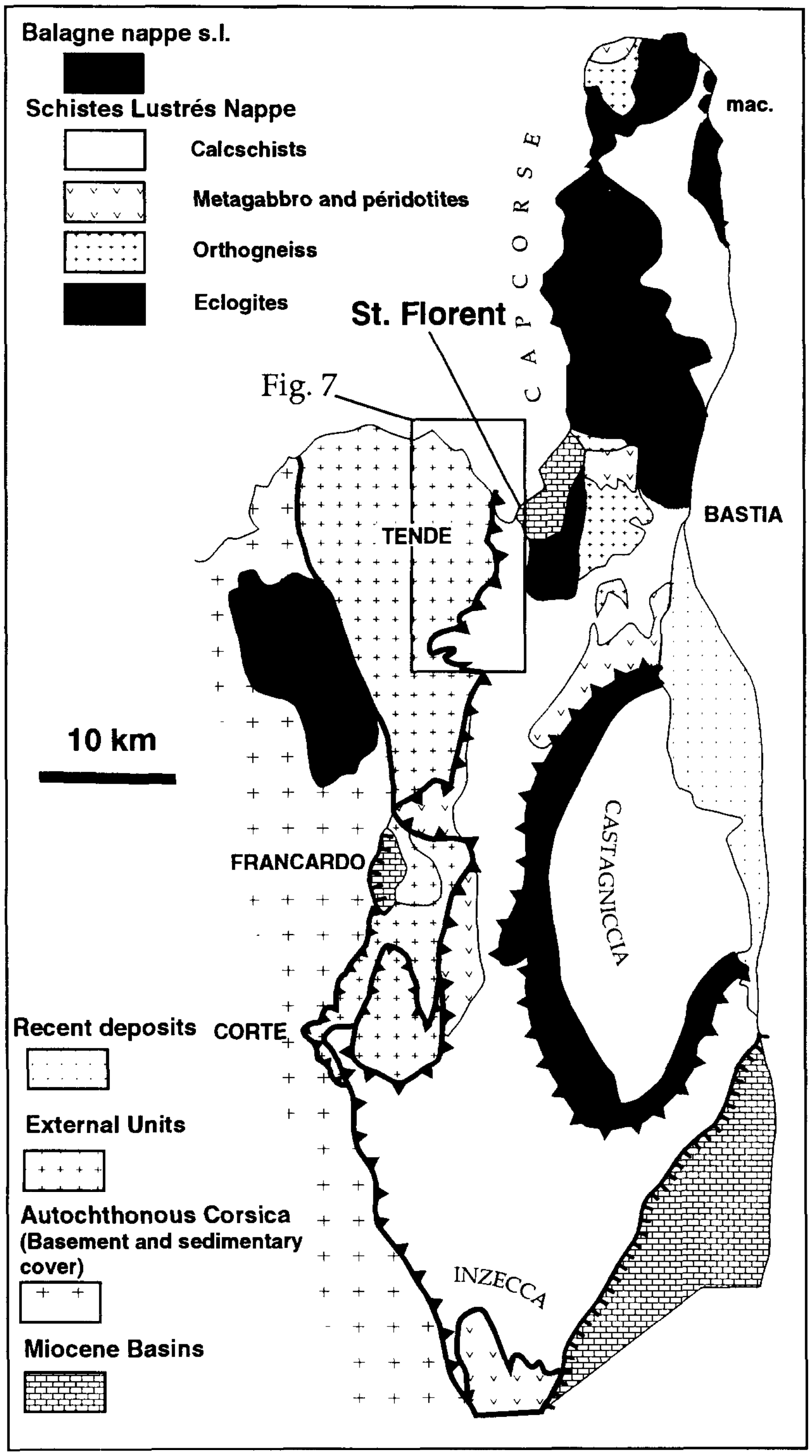

Fig. 2. Simplified geological map of alpine Corsica after Jolivet *et al.* (1990) (the Balagne Nappe is not metamorphosed).

Deformation continued under greenschist facies conditions (D_2) (Table 1) with the activity of shear zones associated with top-to-the-east movements and the development of SE verging folds with an axial planar cleavage (Malavieille 1982, Harris 1984, Warburton 1986, Waters 1989, Jolivet *et al.* 1991, Egal 1992). The latest deformation (D_3) mainly consists of normal and strike-slip faulting (Maluski *et al.* 1973, Egal 1989, Waters 1990). Finally, after the deposition of the St Florent limestones in the Early Miocene, the whole structure was gently folded by N–S trending kilometre scale folds (Faure & Malavieille 1981, Amaudric du Chaffaut 1982) (Figs. 2 and 3). Unlike D_1, the geodynamical significance of D_2 and D_3 is disputed. Three main models (Table 1) have been derived using the observations summarized above: (1) Compression continued during D_2, considered as a backthrusting event and ended with folding (D_3) in the Early Miocene (Harris 1984, Warburton 1986); (2) D_2 started with extension limited to the upper part of the accretionary wedge along ductile normal faults with top-to-the-east sense of shear while compression continued at depth in the way de-

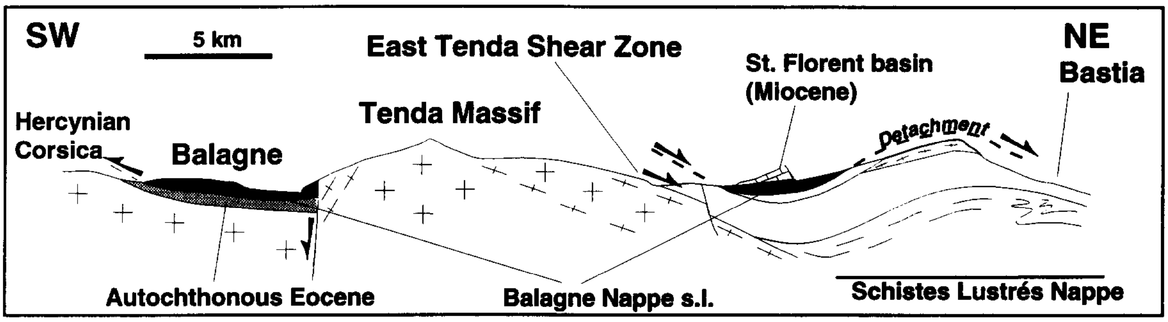

Fig. 3. Synthetic southwest–northeast cross-section at the latitude of Bastia after Fournier *et al.* (1992) (in black: Balagne Nappe *sensu lato*).

Table 1.

Structures	Syn-greenschist shear zones and recumbent folds	Syn- to post-greenschist shear zones and E–SE verging folds with axial plane cleavage	Brittle normal and strike-slip faulting and post-Early Miocene folding
Model 1*		D_3: backthrusting	D_4: last increments of shortening in the crustal wedge
Model 2†	D_2: extension in the upper part of the accretionary wedge	D_3: backthrusting	D_4: last increments of shortening in the crustal wedge
Model 3‡	Post-Orogenic extension	Post-Orogenic extension	D_3: end of exhumation and extension

*Mattauer *et al.* (1981); D_3 is referred to as D_2 in Malavieille (1983); Warburton (1986).
†Waters (1989).
‡Jolivet *et al.* (1990), and this paper.

scribed by Platt (1986). Then, compression re-affected the whole wedge causing backthrusting and SE verging folding. It finally ended (D_3) with open folding of the whole structure in the Early Miocene (D_2, D_3 and D_4 in Waters, 1989); (3) D_2 and D_3 correspond to crustal thinning related to the opening of the Ligurian and Tyrrhenian Basins (Jolivet *et al.* 1990). Model (3) is based on the following observations:

(1) The very sharp basal contact of the unmetamorphosed Balagne Nappe represents a minimum pressure gap of 3 kb and has many characters of a detachment fault.

(2) The eastern margin of the Tenda Massif, where D_2 resulted in pervasive simple shear, appears as a normal shear zone reactivating an early high P–low T thrust plane. This motion is compatible with the later tilt and asymmetric brittle deformation of the St Florent Miocene sediments.

(3) The inversion of sense of shear between D_1 and D_2 can easily be explained by the re-working of D_1 thrusts as normal ductile shear zones. There is no objective reason to interpret some greenschist facies shear zones as backthrusts when others are interpreted as normal sense shear zones.

(4) Regions such as the Basin and Range Province or the Aegean Sea provide examples of long wavelength folds related to extension. Thus the existence of gentle kilometre scale folds and tilt of the Lower Miocene St Florent Basin is not evidence for shortening during the Miocene. They can be formed during extension (roll over structures or isostatic rebound on normal fault) (Wernicke & Axen 1988). Such an interpretation is in agreement with the lack of significant reverse faults in Miocene Basins.

(5) Alpine Corsica is located between two basins (Fig. 1). The Liguro–Provençal Basin contains crust of oceanic affinity (Burrus 1984, Réhault *et al.* 1984). Rifting is known to have begun in the Oligocene (Réhault *et al.* 1984) and continued until the Early Miocene. In Alpine Corsica, an extensional phase, responsible not only for brittle deformation but also for intense ductile deformation, is consistent with such a geodynamical setting.

Most of the data supporting this interpretation have been collected in the region between St Florent and Bastia. This paper presents data concerning D_2 and D_3 over the whole of Alpine Corsica which, integrated at large scale, make us favour model (3). Furthermore, they demonstrate how post-orogenic extension can lead to strain partitioning in the footwall of a major detachment.

D_2 STRETCHING IN THE MIDDLE CRUST

D_2 ductile structures

In this paper, D_2 refers to deformation occurring at the greenschist facies conditions or slightly lower grade. It is best characterized by a small number of large scale shear zones, mapped on Fig. 4, and by small scale kinematic indicators (Figs. 5 and 6). The two major ones are the East Tenda Shear Zone (Waters 1989, Jolivet *et al.*, 1990) and the one that bounds the Castagniccia antiform to the northeast. These shear zones are defined

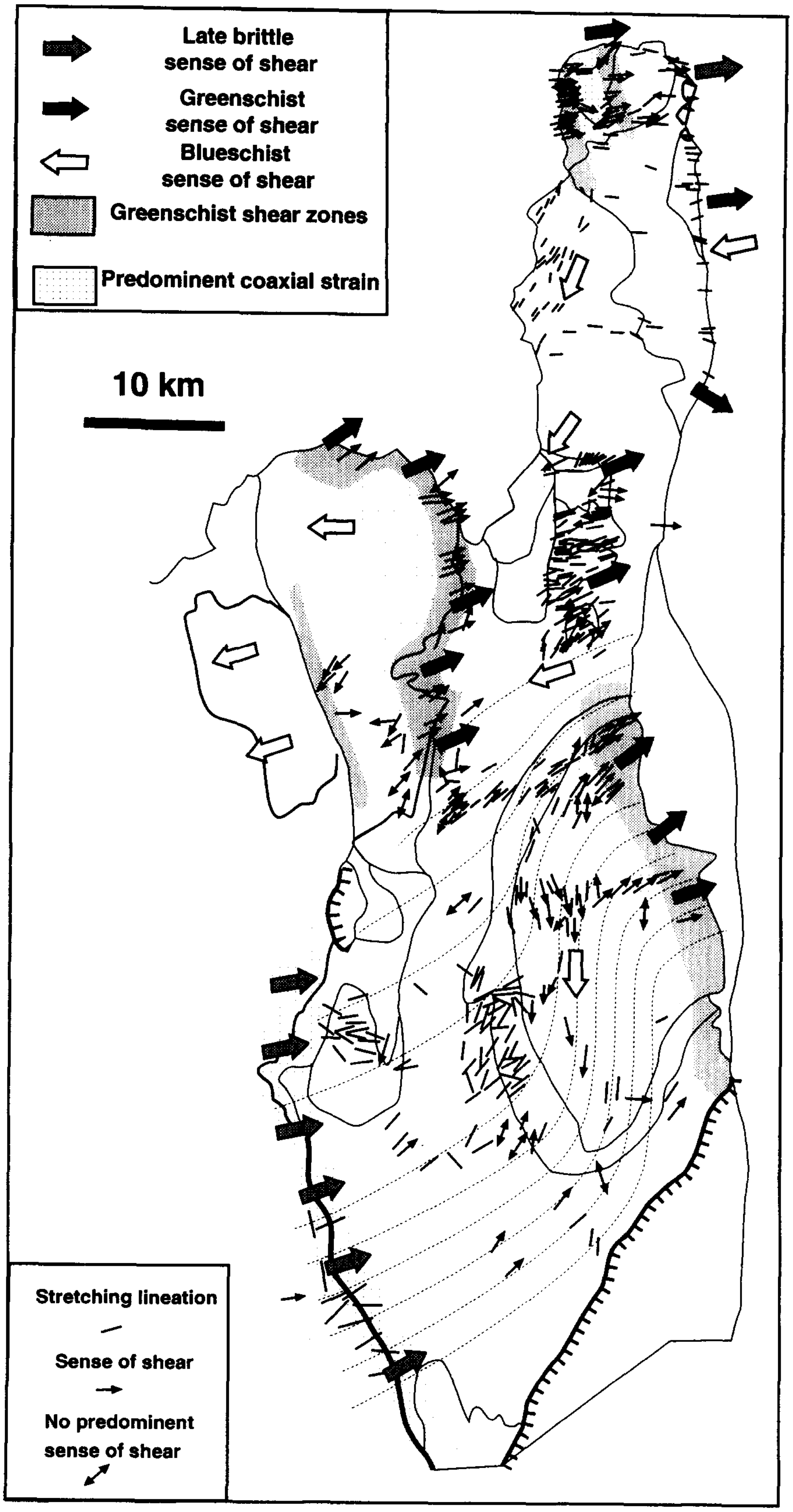

Fig. 4. Structural map of Alpine Corsica. Data from Pequignot and Potdevin (1984), Egal (1989), Harris (1984) and this work. Note in the south the contact between Alpine and Western Corsica is drawn as a brittle normal fault. This point is discussed in the text when D_3 is described.

by an E–NE dipping foliation, a pervasive stretching lineation trending from W–E to SW–NE and consistent top-to-the-east kinematic indicators. Along these shear zones, the retrograde metamorphism of the high *P*–low *T* paragenesis into greenschist facies parageneses is pervasive (Gibbons *et al.* 1986, Waters 1989, Jolivet *et al.*, 1990).

Between the shear zones, D_2 deformation mostly consists of folds with flat-lying–W dipping axial planes, verging E–SE (Fig. 5a). At small scale, a horizontal or W dipping D_2 crenulation cleavage is developed (Figs. 5c & f). There is a general agreement concerning the greenschist facies character of these features, referred to as D_2 by Cohen *et al.* (1981) and Faure & Malavieille (1981) or D_3 by Harris (1984), Warburton (1986) and Waters (1989). D_2 folds were described by these authors as evidence for E verging backthrusts. A component of non-coaxial flow parallel to their axial plane produced slightly curved hinges trending E, but Fig. 5(a) shows that the component of vertical shortening is predominant.

D_2 folds and crenulation cleavage re-worked an earlier foliation and synfolial folds (Figs. 5b & f). These structures can be observed in outcrops within the core of major units where the crenulation cleavage is not too pervasive or did not develop. Figure 4 shows that between large D_2 shear zones, a stretching lineation frequently trends around N20′E, particularly in the core of the Castagniccia antiform. In this region, it is marked by elongated high *P*–low *T* relicts, containing quartz veins and chlorite patches. These north–south lineations are rotated towards southwest–northeast in the vicinity of D_2 shear zones (Fig. 4). At outcrop scale, the related foliation is commonly deformed by D_2 shear bands with top-to-the-east sense of shear trending parallel to the north–south lineation. Therefore, the foliation and lineation clearly pre-date the development of the ductile normal faults and the D_2 crenulation cleavage. The discussion of the geodynamical significance of the north–south stretching direction is beyond the scope of this paper. Despite its surprising trend (N20E), perpendicular to D_1 and D_2 lineations, it has not properly been taken into account in earlier syntheses.

The East Tenda Shear Zone (ETSZ)

A detailed description of D_2 structures along the East Tenda Shear Zone (ETSZ) (Figs. 5d–f and 7) outlines the main characters of finite strain distribution across the major D_2 ductile normal faults.

The core of the Tenda Massif is made of undeformed granodiorite. However, deformation is sometimes localized in high *P* shear zones, a few metres thick, characterized by E–W stretching lineation and top-to-the-west sense of shear (D_1) (Jourdan 1988).

When approaching its eastern boundary the granodiorite becomes more and more deformed and D_1 structures are re-worked by an evolution from syn- to post-greenschist facies (Jourdan 1988, Waters 1989, Jolivet *et al.*, 1990). North of Sorio, D_2 is first defined by outcrop scale folds, similar to the ones found on the east side of the Cap Corse (Fig. 5a). Their axial planes are W dipping and are outlined by a crenulation cleavage S_2 (Fig. 5f). A D_1 crossite-bearing foliation is folded between crenulation planes. A few hundred metres from the boundary, S_2 becomes more pervasive, but is still dipping 30° to the west. S_2 is locally deformed by E dipping shear bands indicating top-to-the-east sense of shear. Approaching the contact with the Schistes Lustrés Nappe, S_2 is progressively rotated to the horizontal and shear bands becomes more abundant (Fig. 5d). In the ETSZ itself, S_2 is developed as an E dipping mylonitic foliation. On S_2 planes, a strong SW–NE stretching lineation is observed. Within the ETSZ shear bands always trend perpendicular to stretching lineation and consistently indicate top-to-the-east sense of shear (Fig. 5d). In the centre of the shear zone, curved folds axes often tend to be parallel to the D_2 stretching lineation, indicating an increase of finite strain.

Even close to the contact, the ETSZ is not a homogeneous shear zone. Figure 7 shows that it is composed of several large scale shear bands. Only the two major ones, 100 m thick, can be mapped in a region covered with dense vegetation. Between these shear zones, a crenulation cleavage is preserved, more or less rotated parallel to D_2 foliation. At outcrop scale, lenses of preserved crenulation cleavage are also observed, of various sizes. Both the size reduction and the progressive rotation of the D_2 cleavage are compatible with increasing shear intensity the contact. The intersection of the crenulation cleavage and the foliation is almost horizontal (Fig. 7). The stretching lineation always lies perpendicular to this intersection (Fig. 7). These geometrical relations are somehow similar to those between *S* and *C* planes on a small scale (Choukroune & Lagarde 1977, Berthé *et al.* 1979). In the same way as the *S–C* angle is reduced when shear strain is increased, D_2 crenulation cleavage tends to become parallel to the mylonitic foliation near the contact. These structures are also similar to an extensional crenulation cleavage (Platt & Vissers 1980). However, the D_2 crenulation cleavage post-dates thrusting events and is closely related in space and is kinematically compatible to ETSZ. Therefore, these D_2 structures can be considered as synchronous as discussed in a later section of this paper. The fact that the crenulation cleavage is deformed by late, more localized, shear bands near the contact (Fig. 5e) and by small scale normal faults, illustrates the progressive character of D_2. It is consistent with unroofing of the Tenda Massif toward the brittle domain.

These observations, summarized in Fig. 8, demonstrate that, in contrast to previous descriptions (Mattauer *et al.* 1981, Gibbons & Horak 1984), the ETSZ is an illustration of how a ductile thrust is re-worked as a normal shear zone (see also Waters, 1989). Away from the main shear zones, planes of flattening of D_1 and D_2 are almost perpendicular and strain intensity is lower. This domain is characterized by the presence of outcrop scale folds in the field. Approaching the shear zone, increasing shear intensity is associated with more pene-

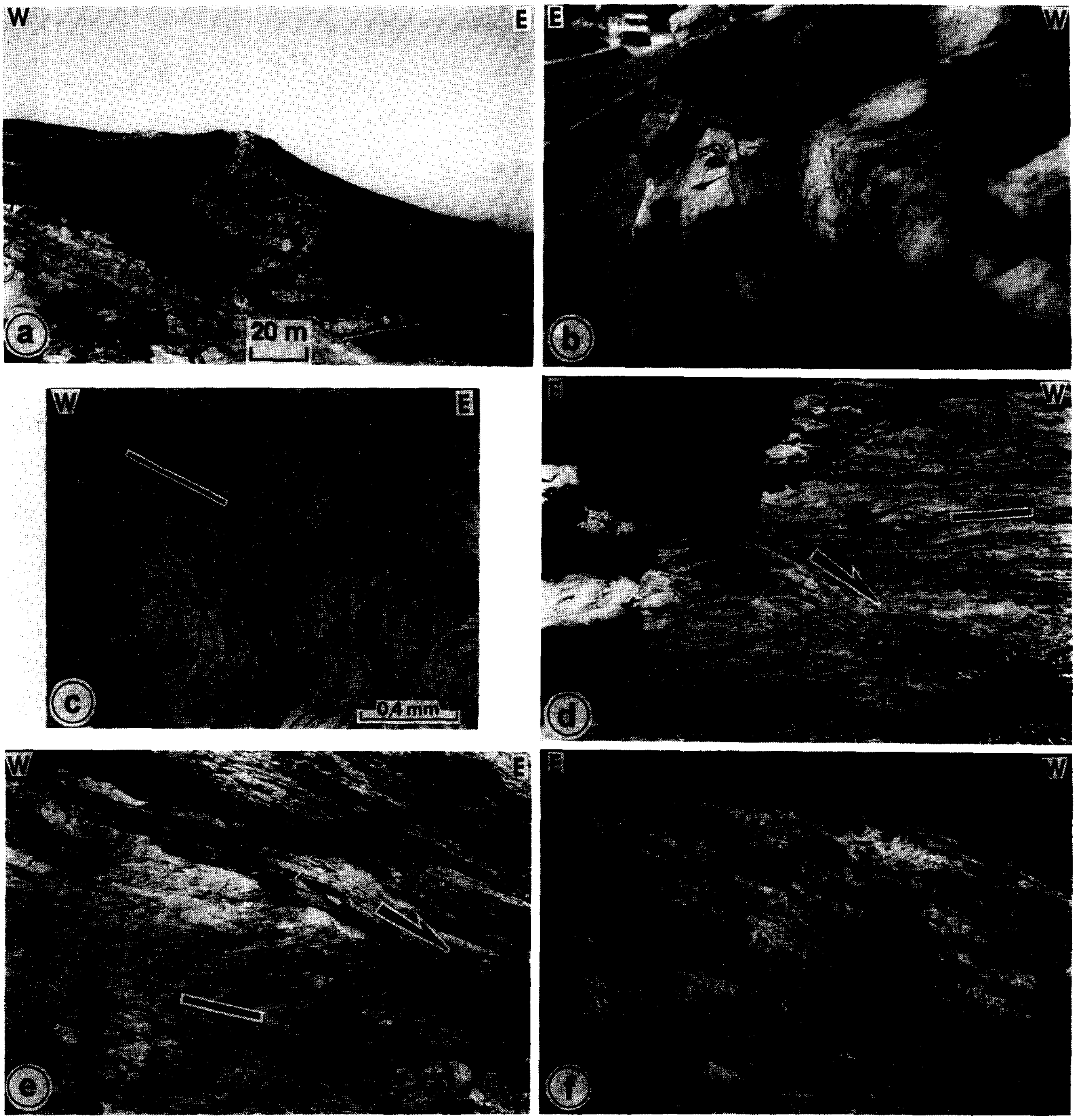

Fig. 5. Variation of deformation pattern along an east–west transect of alpine Corsica: (a) hectometric D_2 folds on the eastern coast of Cap Corse. (b) Detail of (a); D_1 isoclinal fold, refolded by D_2 (lens cap for scale). (c) Thin section showing D_1 blue amphiboles broken by D_2 crenulation cleavage (black minerals in the centre). (d) D_2 shear band below the ETSZ (lens cap for scale). (e) Relation between D_2 crenulation cleavage and D_3 shear bands in the ETSZ (lens cap for scale). (f) D_2 crenulation cleavage in the Tenda Massif (lens cap for scale).

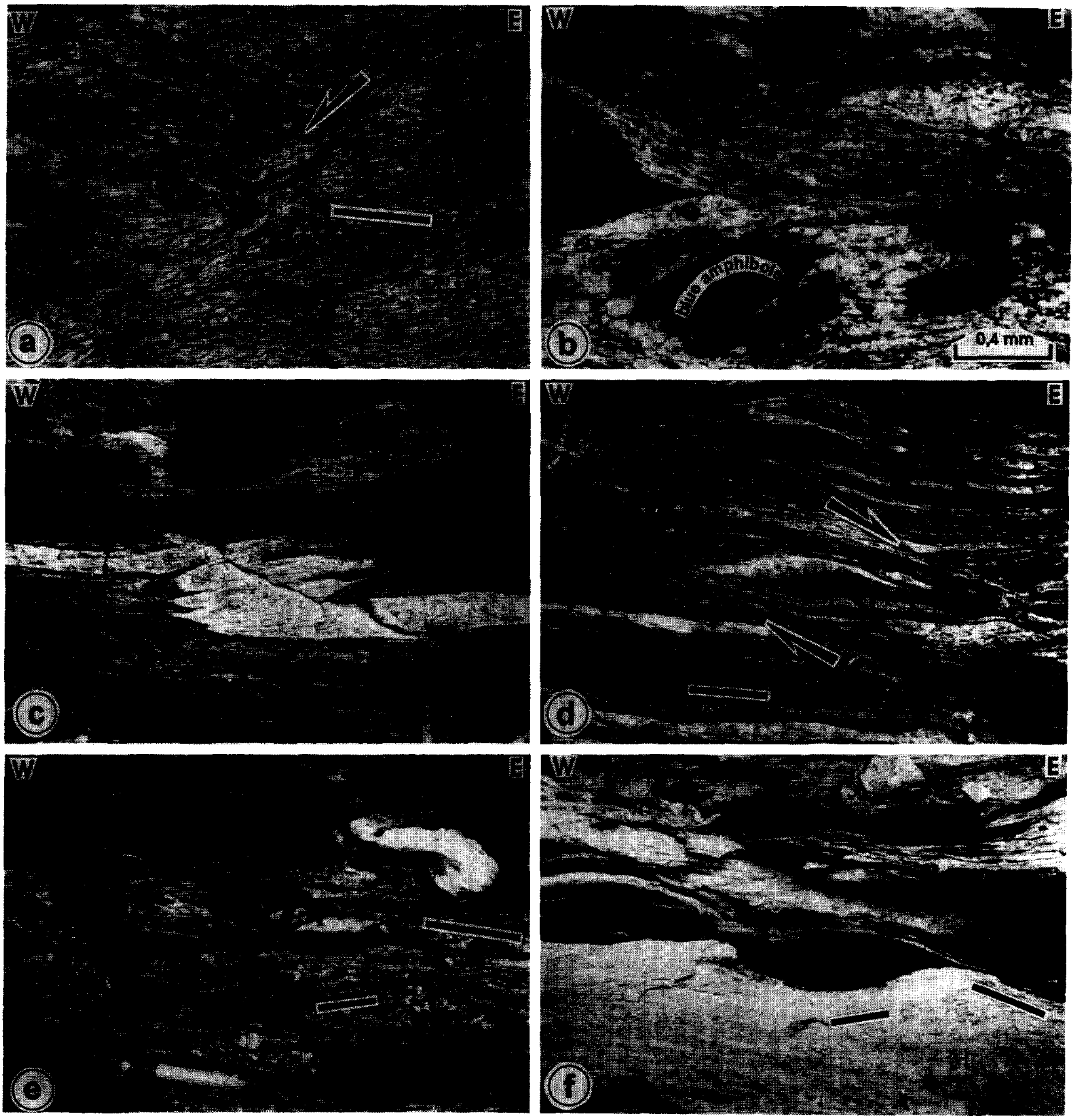

Fig. 6. Aspects of D_2 deformation in Centuri region: (a) top-to-the-west shear band in Centuri orthogneisses (pen for scale). (b) Thin section: broken crossite parallel to D_2 lineation (epidote, chlorite) in Centuri orthogneisses. (c) Fold with minor simple shear component in Centuri Orthogneisses (lens cap for scale). (d) Top-to-the-east shear bands at Monte San Antonino (lens cap for scale). (e) Crenulation cleavage and top-to-the-east shear bands in calcschists (pen for scale). (f) Crenulation cleavage, top-to-the-east shear bands and boudinage in Centuri orthogneisses (lens cap for scale).

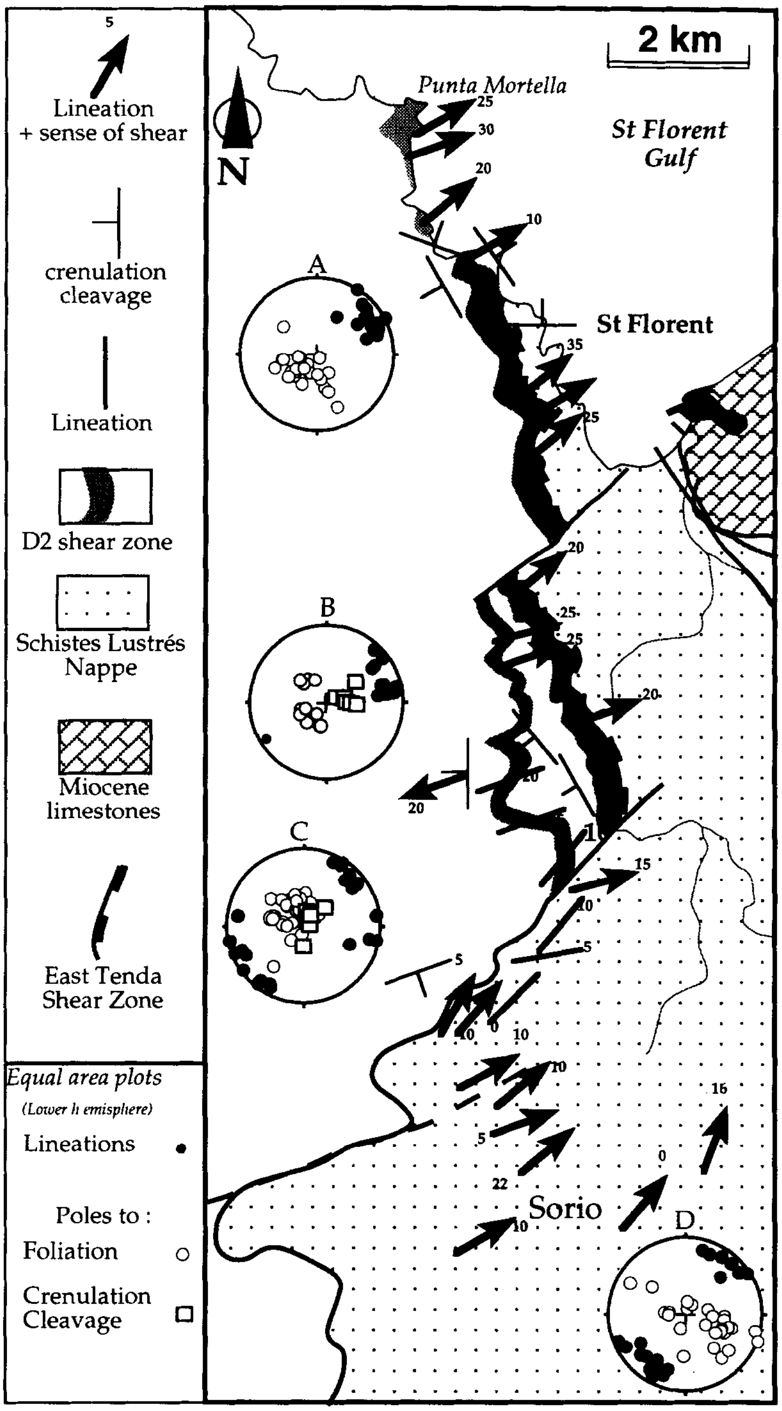

Fig. 7. Detailed structural map of the East Tenda Shear Zone. Stereo-plots A, B and C display data concerning the orthogneisses near the contact with the Schistes Lustrés Nappe, whereas stereoplot D deals with the data within the Nappe. In map view, the southern portion of the ETSZ is deformed by a fault zone trending SW–NE. A dextral strike-slip component of movement along this fault can explain folding (N20° axes) of foliation in the Schistes (plot D) (see also Waters 1990), but a normal one (down to the southeast) has to be advocated to explain the southeastern dip of foliation along the ETSZ (plot C).

trative D_2 crenulation cleavage. The frequent asymmetry of folds toward the east can be linked to the obliquity between the D_1 foliation and D_2 axis of shortening. Close to the contact, D_1 fabrics are so intensely re-worked by D_2 deformation that both phases cannot be easily separated.

The shear zone that bounds the Castagniccia antiform to the northeast displays the same deformation pattern (Fig. 4). However, in this case, the existence of a former thrust cannot be proven.

Evolution of the Centuri region

Deformation in the Centuri region, at the northernmost tip of the Cap Corse, is characteristic of D_2 geom-

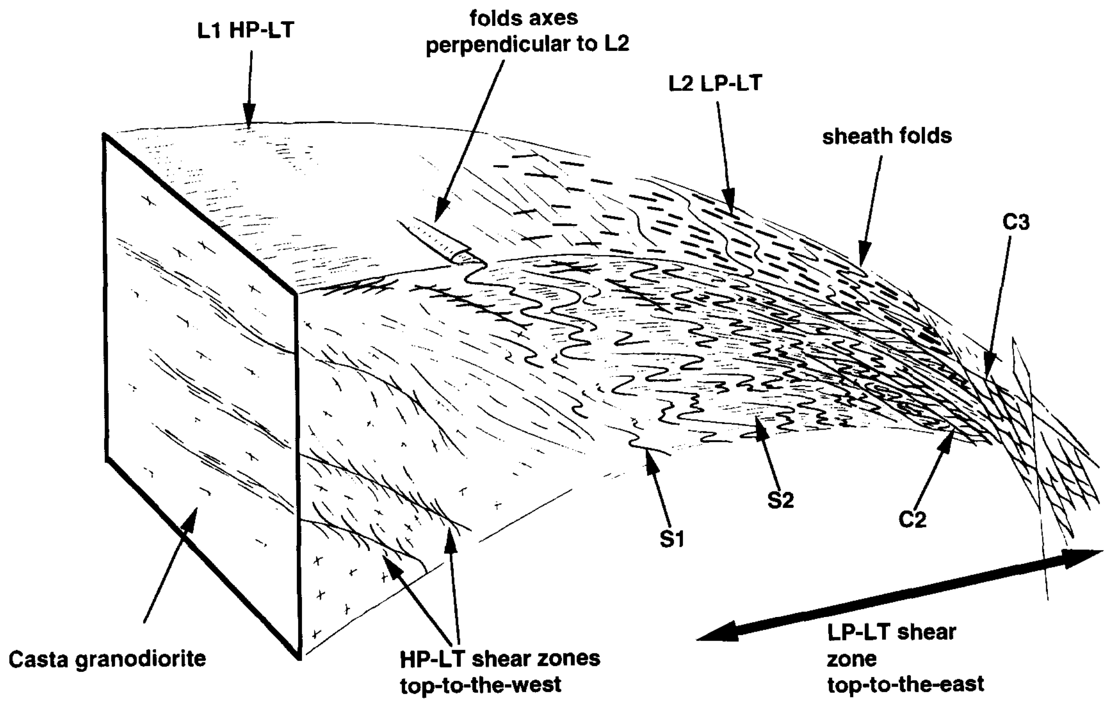

Fig. 8. Block diagram summarizing the main features observed along the East Tenda Shear Zone (see text for explanation).

etry as developed in the Schistes Lustrés Nappe between major D_2 shear zones.

Main tectonic units. Five tectonic units may be defined in Centuri region (Guillou 1962, Ohnenstetter *et al.* 1976, Jackson & Ohnenstetter 1981, Guiraud 1982, Malavieille 1982, 1983, Harris 1984, Lahondère 1988, Lahondère & Lahondère 1988), from base to top (Figs. 9 and 10): (1) calc-schists; (2) metabasites of ophiolitic origin; (3) ortho- and paragneiss of continental origin (Centuri gneiss); (4) ultramafics (strongly foliated serpentinites and the well-preserved Monte Maggiore peridotites); and, at the top of the pile, on the Western coast, (5) small remnants of the Balagne Nappe. Except for (5), the tectonic units presented above are part of the Schistes Lustrés Nappe and exhibit typical low P–high T assemblages and high P–low T relics.

D_2 structures. In the continental basement unit, D_2 is very similar, at a smaller scale, to deformation in the vicinity of the ETSZ. It is localized along shear zones bounding the unit and becomes less penetrative inward (Harris 1984, Waters 1989). Within shear zones, D_2 led to the formation of L–S tectonites with a stretching lineation consistently striking N60°E. Quartz grains are ductilely deformed forming elongated ribbons, whereas K-feldspar is deformed in a brittle fashion and locally replaced by sericite. This type of deformation occurs near the brittle/ductile transition and is coeval with retrogression in the stability field of greenschists. D_2 is also indicated by isoclinal folds and boudinage of basic lenses seen in SW–NE striking planes of outcrop (Fig. 6f). Where D_2 is less penetrative, it produced a W dipping (30°) crenulation cleavage reworking a high P–low T foliation (D_1). South of Centuri in a small orthogneissic klippe, one can observe open folds with a nearly horizontal axial plane parallel to the crenulation cleavage described above, similar to those described several hundred metres away from the ETSZ and on the east coast of Cap Corse (Fig. 5a). These microstructures are syn- to post-greenschist facies metamorphism (Fig. 5c). They re-work D_1 structures and high P–low T associations are only found as relicts. For example, the core of boudins in Fig. 6(f) preserve early glaucophane which crystallized under static conditions. Also, at a larger scale, gradients of retrogression are linked to strain gradients. A cross-section along the coast north of Centuri demonstrates that retrogression increases toward the contact between oceanic and continental units, where deformation is localized (Fig. 10). On this cross-section, S_1 is transposed by S_2 (Fig. 6b), but south of Centuri, within the orthogneisses, S_1 is better preserved and is only folded by the D_2 crenulations.

Within the calcschists unit, D_2 lineations also trend around 60°N and several horizontal or E dipping thin shear zones with top-to-the-east sense of shear can be observed. Folds are tighter than in orthogneiss but still overturned to the east (Harris 1984), with axial planes dipping to the W (dip between 40 and 60°), associated with a crenulation cleavage. Such structures are similar to those observed in the continental basement unit. However, the relations between deformation and metamorphism are more ambiguous, beacause characteristic greenschist facies associations are frequently lacking.

D_2 kinematics

D_2 kinematic indicators (Ghosh & Ramberg 1976, Choukroune & Lagarde 1977, Berthé *et al.* 1979, Platt & Vissers 1980) give both top-to-the-east sense of shear

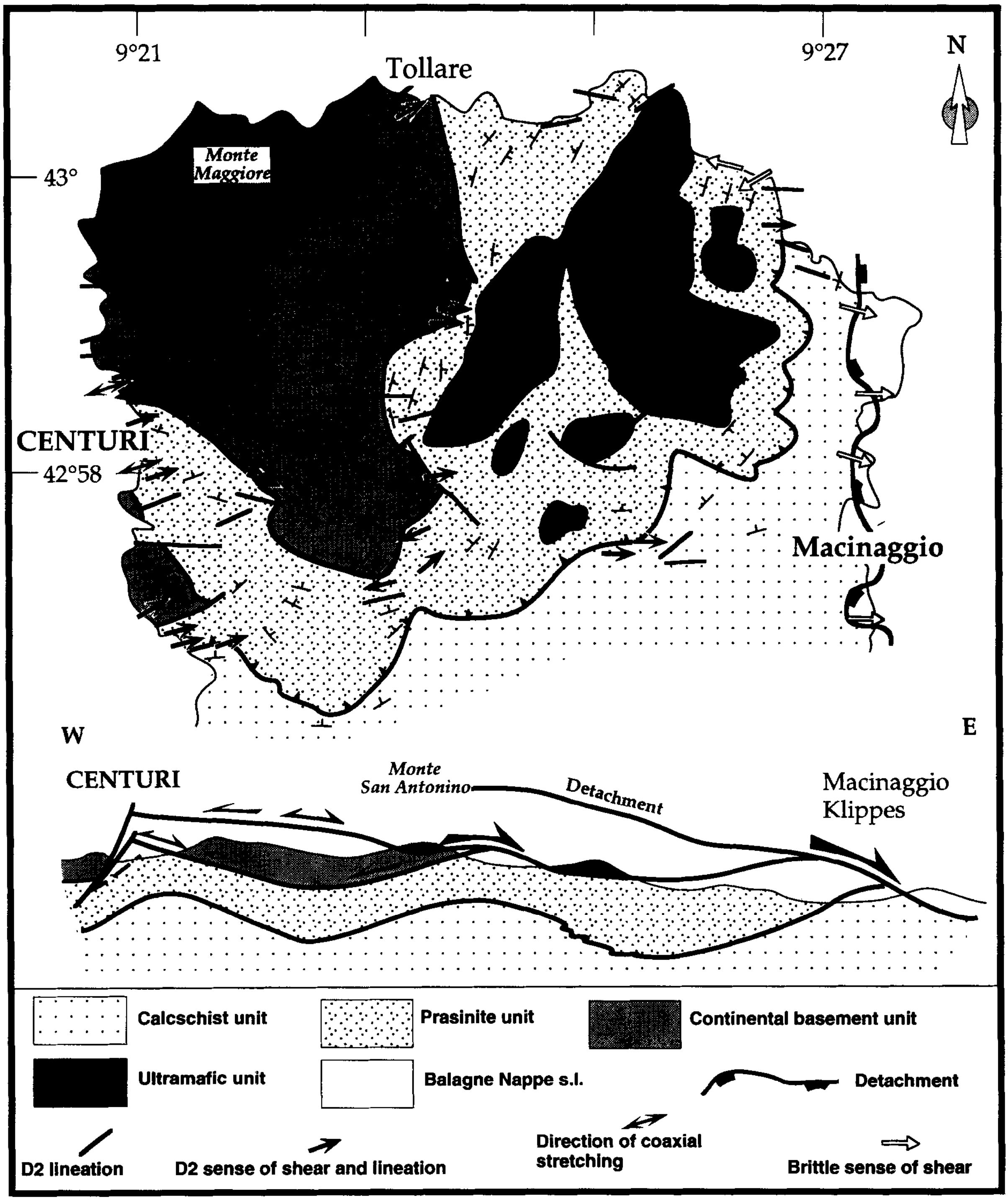

Fig. 9. Geological, structural map and cross-section of Centuri region. Geological contours after Guillou (1962) and personal observations. Coaxial stretching means that at outcrop scale both sense of shear are observed, with sometimes conjugated shear bands (see text for explanation).

(the more frequent: Figs. 6d–f) and top-to-the-west (Fig. 10a). As noticed by Malavieille (1982), these variations are not due to a late stage folding because the sense of shear is similar in both limbs of folds with axes sub-parallel to the lineation.

The continental basement unit shows a peculiar distribution of kinematic indicators. At the base, near Centuri (Fig. 10), D_2 is mostly symmetric: top-to-west (Fig. 6a) and top-to-the east senses of shear coexist (with a slight dominance of the latter) and conjugate sets of ductile shear bands are common (Harris 1984). This is different from the eastern part of the unit, where gneisses are cut out tectonically by overlying ultrabasites (Fig. 9). There, S_2 is rotated toward the boundary of the orthogneiss unit, compatible with the top-to-the-east sense of shear that is systematically observed below the upper contact (Fig. 6d).

It is generally agreed that the predominant sense of shear is representative of the movement direction along a given shear zone. ‘Conflicting’ kinematic indicators

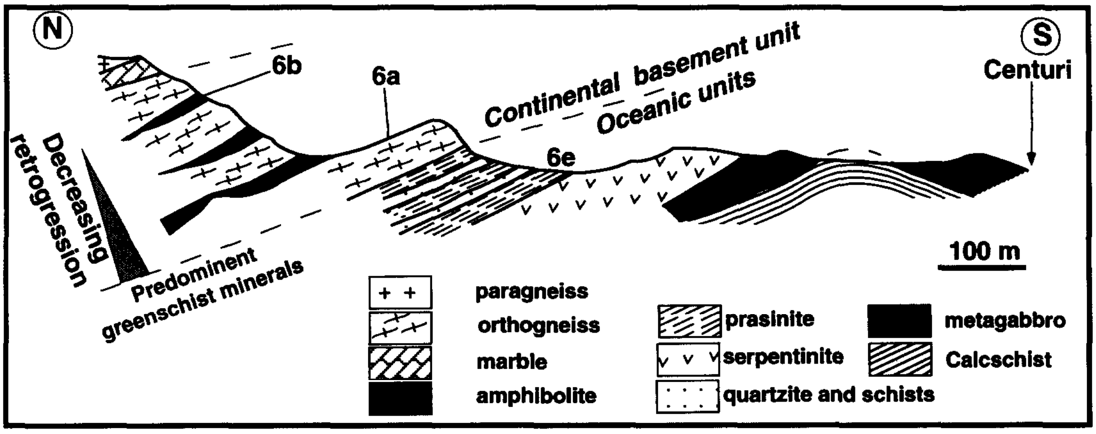

Fig. 10. Cross-section along the west coast, from Centuri toward the continental basement Unit. Numbers refer to figures of this paper. These figures show some examples of shear sense criteria indicating opposite senses of movement along this cross-section, even in a single unit.

are sometimes supposed to be non-reliable or caused by small heterogeneities that locally complicate the deformation pattern. In this case, a slightly different approach is used because spatial variations are significant and consistently described by different types of D_2 kinematic indicators (shear bands, pressure shadows and quartz C-axes fabrics) (Malavieille 1983). Shear sense criteria are taken to be representative only of the kinematics on a mesoscopic scale and its variation is considered to be informative of the geometry of deformation on a larger scale. A classification according to the dominant sense of shear at outcrop scale: (1) top-to-west; (2) top-to-the-east; and (3) both senses on the same outcrop (Fig. 9) is used to qualitatively describe spatial variations of shear sense.

This approach demonstrates that during D_2 the continental basement unit suffered asymmetrical boudinage (Fig. 6). D_2 is highly non-coaxial on the eastern side, where a pervasive shear zone with top-to-the east shear is observed. Toward the west, deformation is more coaxial. This is indicated by conjugate shear bands, development of D_2 crenulation cleavage and folds. At the map scale, deformation is asymmetric and top-to-the-west shear zones are scarce. This asymmetry is consistent with a dip toward the W of the crenulation cleavage and the E vergence of large scale folds (Fig. 5a). The same geometry can be observed on a small scale. In Fig. 6(f), the asymmetry of deformation is clear, with a top-to-the-east sense of shear, and stretching is marked by elongate amphibolitic boudins which are asymmetrically disrupted by E dipping shear bands. Two other types of structures are also present at this exposure: (1) folds with an axial plane parallel to the foliation and eastward asymmetry (Fig. 6c); and (2) a W dipping crenulation cleavage between shear bands (Fig. 6f) rotated toward the shear bands. At this scale, the distribution of microstructures suggests asymmetric boudinage. The comparison between the east side (intensely sheared) and the west side (more coaxial deformation) of the continental basement unit strongly suggests that this unit has also suffered asymmetric boudinage and that the same distribution of deformation exists from outcrop scale, up to map scale.

Spatial variation of D_2 fabrics at the scale of Alpine Corsica

Strain variation along east–west cross-sections. Observations of the ETSZ and the Centuri region give local illustrations of the structure in Alpine Corsica along an east–west cross-section, parallel to the D_2 stretching lineation. Beneath the detachment fault, well defined on the east coast, two zones of predominant coaxial deformation and minor eastward shear (Cap Corse and Tenda Massif) are separated by a ductile normal fault characterized by pervasive top-to-the-east shear (Figs. 4 and 11). The Centuri region shows that this distribution is observed at all scales between major shear zones (Fig. 11). This demonstrates that D_2 corresponds to asymmetric boudinage of the whole middle crust.

Variations of D_2 and metamorphism from south to north. Most of the observations concerning D_2 have been made in the north of Alpine Corsica. To the south, D_2 structures are less pervasive and D_1 structures are better preserved. This is especially evident south of Corte, where the main anisotropy in outcrops is related to D_1 (Counas 1986). In contrast with the D_2 planar anisotropy, S_1 there is steeply dipping and D_2 is recorded only by gentle folds corresponding to vertical shortening. In this regional, although a top-to-the-east sense of shear related to D_2 is observed, no major D_2 shear zones are seen (Fig. 4). Along the Alpine front, S_2 is weaker than along the ETSZ and D_1 structures are well preserved (Counas 1986). Therefore, a finite strain gradient exists for D_2 from south to north. It is associated with the preservation of earlier structures in the core of the Castagniccia antiform (the north–south lineation for example) and with a strong northward increase of retrogression.

Figure 12 shows a map of the distribution of metamorphic minerals in metasediments of pelitic composition (after Goffé in preparation). Observations in metabasites suggest a northward increase of the retrogression blueschist into greenschist facies assemblages (Jolivet *et al.* 1990). Metasediments are most affected by this retrogression as illustrated by Fig. 12. The southern part

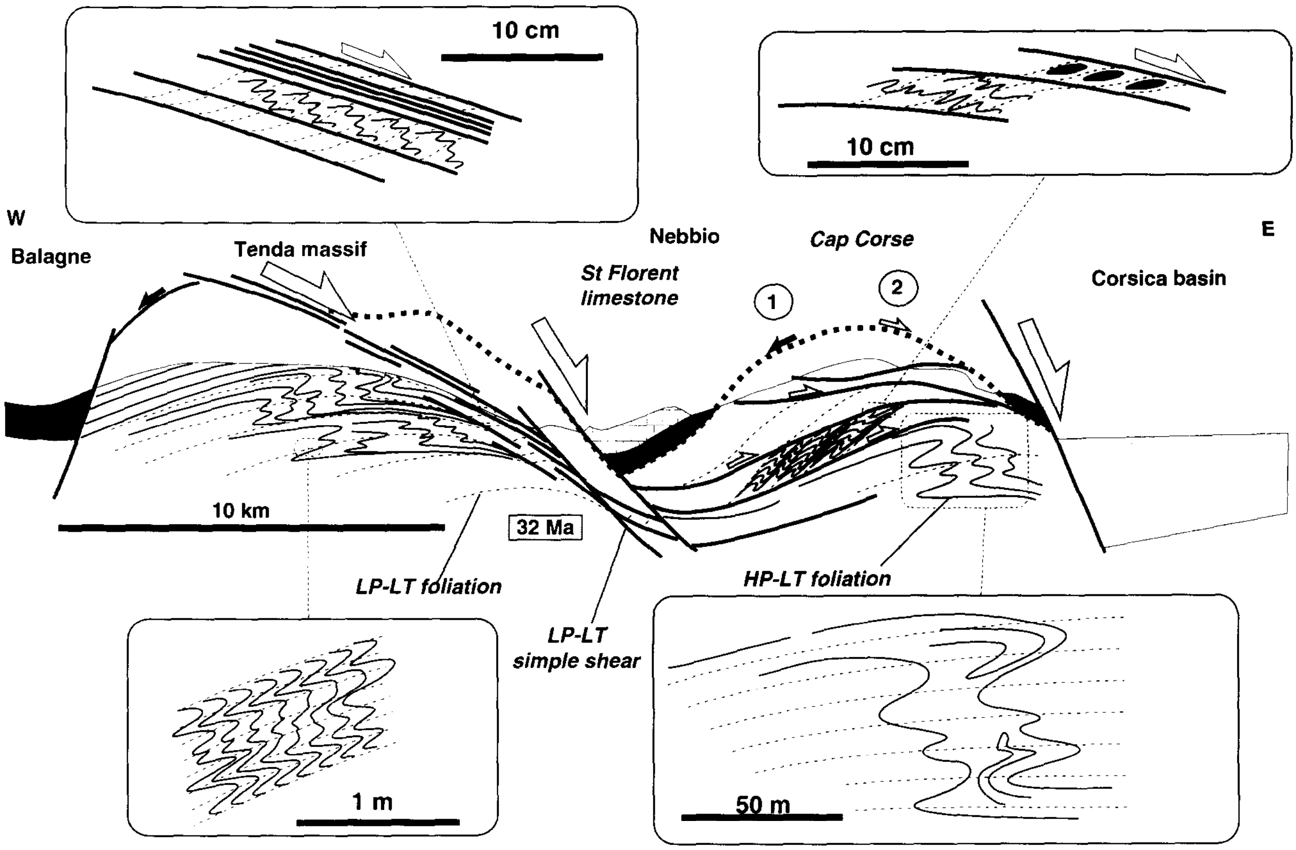

Fig. 11. Synthetic cross-section of alpine Corsica showing the re-working of the high P–low T foliation by extensional structures. Interpretation of the structure of alpine Corsica at various scales.

of Alpine Corsica wholly or partially preserved high P minerals Mg/Fe-carpholite and lawsonite are well preserved south of Corte, but become more and more retrogressed toward the north. Between Bastia and Centuri, only pseudomorphs after carpholite are found. This progressive retrogression also corresponds to a variation in the breakdown products of Fe/Mg-carpholite. South of Corte, Fe/Mg-carpholite was replaced by white micas and chlorite whereas retrogression led to the formation of albite further north. According to Goffé & Vidal (1992), this is symptomatic of the shape of the decompression P–T path, albite appearing only if temperature increases during decompression. In the north, decompression is therefore coeval with heating. Such temperature increase has been described in metabasites (Waters 1989) with a temperature peak near 450°C. South of Bastia it is not observed (Fournier *et al.* 1991) and south of Corte the preservation of Fe/Mg-carpholite rather implies a decreasing temperature during decompression (Goffé & Velde 1984, Gillet & Goffé 1988).

Comparison between Figs. 4 and 12 demonstrates that the two major shear zones shown in Fig. 4 are located in regions almost devoid of preserved high P minerals. On the other hand, high P minerals are preserved in regions where D_2 is not pervasive, for example south of Francardo and Corte and especially along the margins of Alpine Corsica that are not highly ductilely re-worked. Therefore, a relationship between the presence of D_2 shear zones and the degree of retrogression in the greenschist facies exist on a large scale.

D_3 STRETCHING IN THE UPPER BRITTLE CRUST

Detachment and normal faulting

The most important brittle fault is the basal contact of the Balagne Nappe. At the base of Macinaggio Klippes, in Centuri region, it is very sharp and occupied by a fault gouge. Riedel shear asymmetry shows that the hanging-wall has moved to the east. This contact, which cuts off the upper part of the metamorphic complex described above, is the detachment itself (Jolivet *et al.* 1991). A large, E dipping normal fault bounds the large Mio-Pliocene Basin found on the east coast of Alpine Corsica (Fig. 2), the western extension of the Corsica Basin.

Brittle re-working of the thrust front

The main structural boundary in Corsica is the Alpine thrust front. On the basis of observation of small scale strike-slip faults (Maluski *et al.* 1973, Waters 1990), it is generally agreed that it has been re-worked as a strike-slip fault. This major structural boundary is one of the main topographic features of Corsica (Fig. 13). Between Corte and the Tenda Massif it corresponds to a prominent scarp trending N–S, with a mean dip of 17° toward

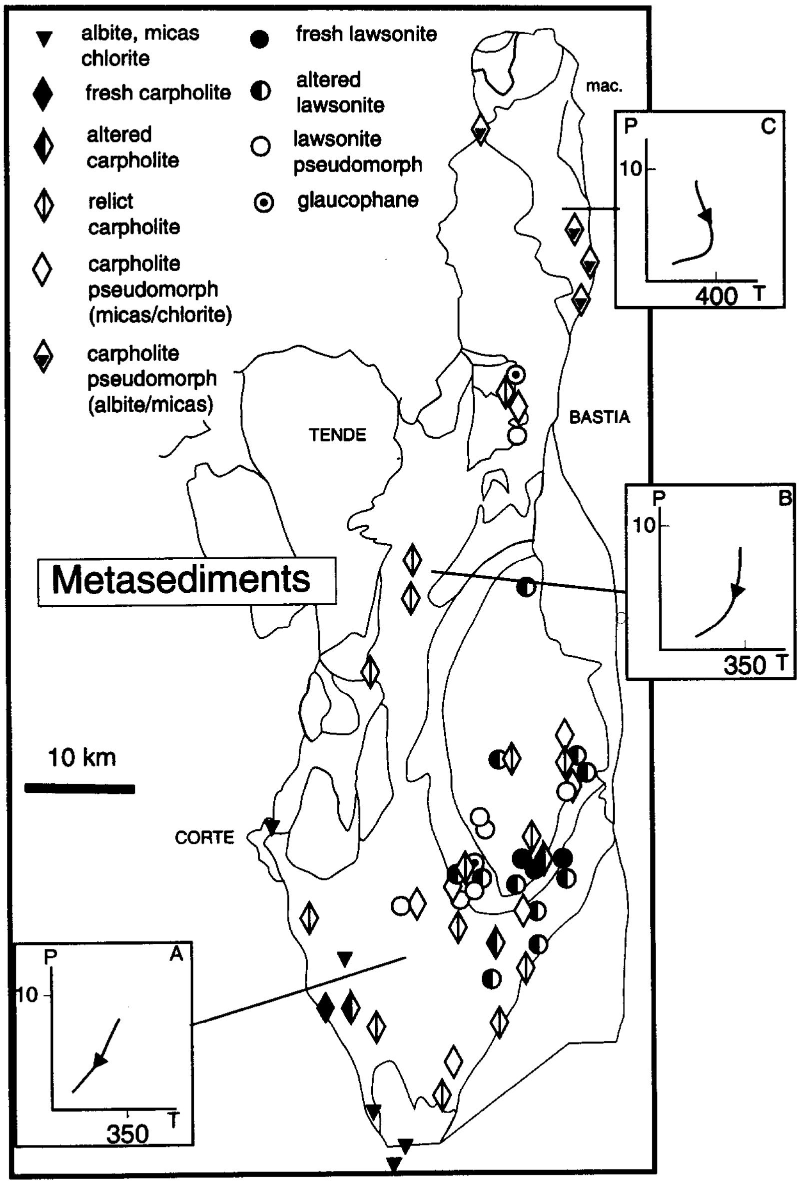

Fig. 12. Main occurrences of high *P*–low *T* minerals (After Goffe in preparation). Symbols refer to the grade of replacement of high *P*–low *T* mineral by chlorite, muscovite, paragonite and illite. Fresh: the mineral is wholly preserved in hand specimens; altered: it is partially replaced but still observed in hand specimen; relict: it is only observed as relict under optic microscope in thin section; pseudomorphs: it is not present, but macroscopic and microscopic shapes are still recognized. (A), (B) and (C): schematic *P–T* paths depending on the degree of preservation of high *P*–low *T* minerals and the pseudomorphs after Fe/Mg-carpholite (see text for explanations).

the E. West of it, the mean elevation is 1000 m, whereas it is less than 500 m in the east. As a result, thrusted units are at a lower elevation in eastern Corsica than undeformed Hercynian rocks of western Corsica. Such a morphology strongly suggests that this relief is due to one or several normal faults. This can be confirmed by the observation of numerous small scale normal faults in its vicinity with the same trend, by the deposition of Miocene sediments on its hangingwall and by the tilt toward the west of strata in the Francardo Miocene Basin. If horizontal movements cannot be ruled out, large vertical displacements have at least to be taken into account.

Apparently, tectonics in the brittle domain has been dominated by extension (see also Egal 1989, 1992). This is not uncompatible with the existence of strike-slip faults (Waters 1990) as Gennesseaux *et al.* (1989) have shown that rifting in the Ligurian Sea included transcurrent movements.

Large scale folding

The present day structure of Alpine Corsica is influenced by late large scale open folds (Fig. 3) (Faure & Malavieille 1981, Amaudric du Chaffaut 1982). They can easily be related to the activity of the large scale normal faults: antiforms are always located between major normal faults trending parallel to fold axes. Following Jolivet *et al.* (1990) (see Table 1), this folding event is interpreted in this paper as a consequence of extension. The lack of small scale reverse faults in Miocene basins strengthens this interpretation.

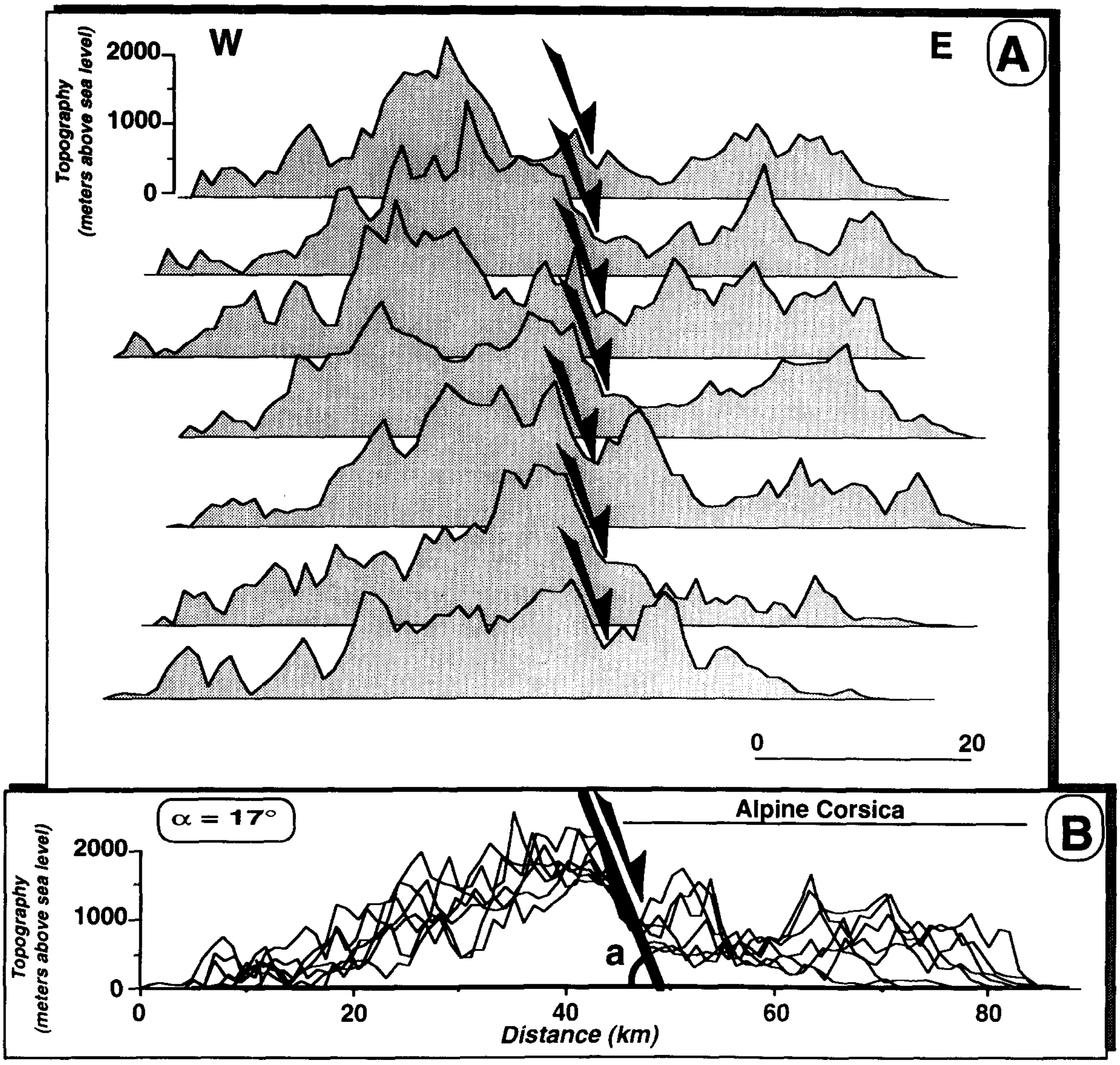

Fig. 13. West–east topographic profiles crossing the whole of Corsica. (A) Profiles spaced every 5.5 km, from the south of the Tenda Massif to the north of Inzecca. (B) Same profiles as in (A), but shifted along an east–west direction to make the scarp coincident.

PROGRESSIVE EXTENSION

Regional scale boudinage associated with an evolution towards more superficial P–T conditions of the whole structure (metamorphism and deformation style) is further evidence of the existence of pervasive ductile deformation (D_2) during extension in Alpine Corsica besides that already mentioned in Jolivet *et al.* (1990). D_2 and D_3 can be interpreted as the result of stretching of a previously thickened crust.

The post-high P–low T history corresponds to the progressive unroofing of ductile crust. The deepest extensional deformation began in greenschist facies conditions. At this depth, S_2 was formed, with almost complete retrogression of high P–low T assemblages in northern Alpine Corsica. The D_2 finite geometry can be described as an asymmetric boudinage of competent units. Non-coaxial flow was concentrated on normal ductile faults. In between, the deformation mostly produced gently W dipping crenulation cleavage and almost horizontal shear zones associated with conjugate shear bands characterizing an important coaxial vertical shortening compatible with extension. This history was recorded in the footwall of the basal contact of the Macinaggio Klippes and Balagne Nappe. During the activity of this detachment, the ductile crust was unroofed and progressively entered the brittle field where observed deformation ended. The activity of large scale normal faults induced an isostatic re-equilibration with vertical shear as shown by Wernicke & Axen (1988). Rare structures, such as steep and narrow shear zones, steep reverse kink bands and major long wavelength folding, which post-date D_2, can be interpreted easily as direct consequences of such a re-equilibration (Bartley & Fletcher 1990). Finally, one can note the same top-to-the-east sense of shear from ductile to brittle structures, with E dipping normal faults.

Metamorphic and structural data demonstrate that D_2

was more pervasive in the north of the island. This gradient of deformation is independently revealed by the deepening of Miocene basins (continental deposits in the Francardo Basin and shallow marine deposits in the St Florent Basin), by northward widening of the western margin of Corsica (Gennesseaux *et al.* 1989) and northward shallowing of the Moho (32–22 km) (Hirn & Sapin 1976, Ansorge *et al.* 1992). The gradient of greenschist facies retrogression toward the north is parallel to the transition from mostly brittle to mostly ductile deformation, and D_2 occurred at higher temperature in the north.

In Corsica, stratigraphic data still provide the best control on the timing of deformation events. Compression affects auchtonous Eocene deposits and high *P* minerals developed in Eocene sediments (Bézert & Caby 1988). Preceding sections have shown that Burdigalian limestones of St Florent Basin were deformed during extension (D_3). D_3 structures can then be associated with the opening of the northern Tyrrhenian Sea where rifting began in the Middle Miocene along N–S trending normal faults (Zitellini *et al.* 1986).

Our interpretation of D_2 in terms of crustal thinning could be tested by radiochronologic dating of D_2 structures. $^{39}Ar/^{40}Ar$ ages are quite variable, which is not surprising giving the variations the D_2 intensity. Ages range between 40 and 35 Ma (Maluski 1977). Along the ETSZ, ages as young as 33 Ma are found (Jourdan 1988). The youngest apatite fission track age is 29 Ma (Mailhé 1982). This indicates that Alpine Corsica underwent a rapid exhumation around 30 Ma. This age compares well with the inception of rifting of the Ligurian Sea around 30 Ma (Fig. 1) dated by stratigraphy of the synrift sediments and radiochronological ages of interbedded lava flows (Burrus 1984, Debrand-Passard & Courbouleix 1984, Réhault *et al.* 1984) or apatite fission tracks on the basin flanks (Morillon & Sosson 1993; 35–30 Ma). Although ages of D_2 structures are still imprecise, D_2 can be related both kinematically and chronologically to the rifting of the Ligurian Sea.

DISCUSSION AND CONCLUSION

Relation between coaxial and non-coaxial flow

This paper shows that in Alpine Corsica, a detachment unroofed a middle crust internally deformed during extension. This deformation (D_2) corresponds to the superposition in space of two modes of deformation, coaxial and non-coaxial flow, whereas the detachment is a zone of highly localized, non-coaxial flow.

Progressive unroofing is accompanied according to Miller *et al.* (1983) by a progressive localization of deformation. Such a progressive localization is, in Corsica, indicated clearly in the latest stages: steep shear zones which cut across the major foliation are themselves cut by normal brittle faults. In the ductile field, the relation between zones of coaxial and non-coaxial flow are rarely visible, except at a small scale. This model, however, predicts that ductile shear bands should always cut flattening planes such as the crenulation cleavages described. In the field this is rarely observed. Instead of a progressive localization we propose that the boudin-like finite geometry is the result of partitioning of strain in the middle crust within or immediately below the brittle-ductile transition zone. Several observations support this idea:

(1) Vertical coaxial shortening appears to be penetrative at different levels in the crust. Late folds with subhorizontal axial planes even exist as late features in the autochthonous Eocene sediments (Egal & Caron 1988, Egal 1992) which were never buried to great depth. In addition, a sub-horizontal dissolution cleavage characterizes the deformation of Miocene limestones (Egal & Caron 1988). It has the same significance as the D_2 crenulation cleavage at ductile levels.

(2) Pre-existing planar heterogeneities must have played a role early in the extensional deformation as planes of weakness. Early thrusts were reactivated as ductile normal faults (the ETSZ, for example). Ductile reactivation began early in the process of extension and continued until the inherited thrusts reached superficial levels. This is confirmed by the fact that the same greenschist facies minerals are deformed in the shear zones and in the S_2 crenulation cleavage. Therefore, movement along discrete shear zones occurs at the same level as vertical coaxial shortening, as far as can be determined from mineral assemblages.

(3) Variations in shear sense along the boundaries of Centuri gneisses correspond to boudinage of a competent level, a type of deformation also characterized by vertical coaxial shortening within boudins and non-coaxial flow along the boundaries. Such a heterogeneous distribution of structures described at outcrop scale is illustrated here at the scale of Alpine Corsica (Fig. 11). Corsica itself can be regarded as a crustal-scale boudin (Moho at 30 km depth) between two basins with shallower Moho (from 20 to 5 km) (Morelli *et al.* 1977).

Data on the greenschist mineral assemblages give limits for the depth at which the ductile deformation took place. Both pressure and temperature for respectively admissible densities and geothermal gradient indicate depth of about 15 km. Seismological studies have shown that, in regions of active extension (Aegean sea), deformation of the brittle crust is achieved along steep normal faults (dip = 60°). In those cases, a gently dipping plane of low seismic activity is seen in the brittle–ductile transition zone at the base of a pair of conjugate normal faults. This geometry ensures movement compatibility (King *et al.* 1985). The megaboudinage described in this paper can be interpreted as the result of the deformation at the base of tilted blocks and the seismic plane described by King *et al.* (1985) can be envisioned as a crustal shear band similar to the ETSZ (Fig. 14). In this scheme, the major ductile normal faults observed in the field correspond to the seismic plane, the continuation of normal faults at depth. Coaxial flow within the boudins can accommodate internal defor-

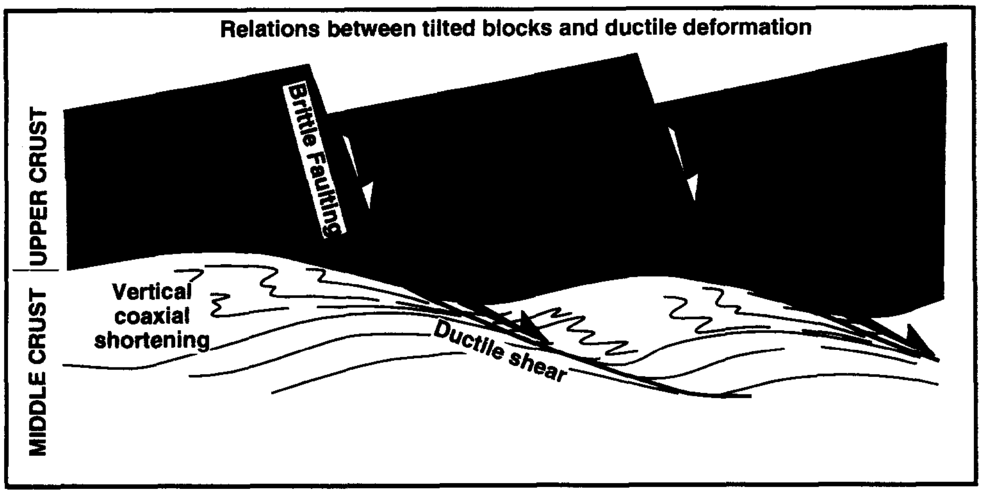

Fig. 14. Relation between crustal-scale shear bands in the ductile field and bloc tilting in the brittle domain. Geometry in the ductile domain correspond to D_2 deformation pattern; relation with brittle domain is discussed in the text. Brittle deformation corresponds to D_3 in this paper.

mation within the tilted block. It is worth noting that the typical width of the domain of coaxial flow (10–20 km) and the length of ductile shear zones (20 km) are very similar to the width of major tilted blocks and length of major normal faults, respectively, as given by geophysical data in adjacent marine areas (Gennesseaux *et al.* 1989) and in Greece in a similar geodynamic setting (Roberts & Jackson 1991). This interpretation explains the existence of Miocene basins in the footwall of every major D_2 shear zone where stretching is concentrated, and the similar asymmetry of major ductile shear zones and E dipping normal faults.

Crustal-scale strain partitioning

The distribution of deformation between shear zones and domains of coaxial flow at all scales (Fig. 11) can be compared with the *S–C* fabric described at a small scale in orthogneiss (Berthé *et al.* 1979). The ETSZ could be envisioned as a pluri-km *C*-plane and the crenulation cleavage axial plane and east-verging open folds symptomatic of shortening, as *S*-planes. However, if one considers a set of these crustal-scale shear bands within the middle crust, their position will surely impose a rigid rotation during extension, and they are then closer to *C'*-planes. But *C'*-planes are late features in a shear zone. The comparison with 'extensional crenulation cleavage' does not hold either because of the contemporaneity of shear bands and crenulation cleavage. To avoid any misunderstanding and confusion with above-cited structures, we choose to name these large scale structures *crustal-scale extensional shear bands*.

Carmignani & Kligfield (1990) described extensional deformation in the footwall of detachment faults in the Alpi Apuane (northern apennines, Italy) and have shown that extension is achieved mostly by the activity of conjugate shear zones. They suggested that deformation at the ductile–brittle transition is characterized by megaboudinage and proposed to generalize this model at lower crustal levels. Observations in Alpine Corsica support this model, showing that in middle crust this type of boudinage exists, albeit with a different style: shear zones are more gently dipping and wider, with more penetrative vertical coaxial shortening in between.

The deformation that we see in Corsica with its crustal scale shear bands has been preserved probably because of a limited finite extension within the lower plate. In the Norvegian Caledonides extension led to the exhumation of eclogites (Séranne & Séguret 1987, Andersen & Jamtveit 1990). Finite extension is thus far greater than in Corsica, where metamorphic rocks where uplifted from depth of 10–20 k only, and a more intense finite shear strain is expected along the detachment in Norway. Séranne & Séguret (1987) and Andersen & Jamtveit (1990) described the deformation in Norway as concentrated in a thick zone with unambiguous consistent kinematics indicators throughout. This is what one could expect to see in Alpine Corsica had finite shear strain been stronger, leading to a rotation of S_2 parallel to the major ductile normal fault and to the generation of a denser array of shear bands parallel to it. Crustal-scale structures described in Corsica can, therefore, be considered as representative of the early evolution of a metamorphic core complex.

REFERENCES

Amaudric du Chaffaut, S. 1982. *Les Unités Alpines à la Marge Orientale du Massif Cristallin Corse*. Presses de l'École Normale Supérieure, Paris, 15 pp.

Andersen, T. B. & Jamtveit, B. 1990. Uplift of deep crust during orogenic extensional collapse: a model based on field studies in the Sogan–Sunnfjord region of Western Norway. *Tectonics* **9**, 1097–1111.

Ansorge, J., Blundel, D. & Mueller, S. 1992. Europe's lithosphere—seismic structure. In: *A Continent Revealed—The European Geotraverse* (edited by Blundel, D., Freeman, R. & Mueller, S.). Cambridge University Press, UK, 33–70.

Bartley, J. M. & Fletcher, J. M. 1990. Tertiary extension and concentration of lower-plate rocks in the central mojave metamorphic core complex, southern california. *Tectonics* **9**, 521–534.

Berthé, D., Choukroune, P. & Jegouzo, P. 1979. Orthogneiss, mylonite and non-coaxial deformation of granites: the example of the South Armorican Shear Zone. *J. Struct. Geol.* **1**, 31–42.

Bézert, P. & Caby, R. 1988. Sur l'âge post-bartonien des évènements tectono-métamorphiques alpins en bordure orientale de la Corse cristalline (Nord de Corte). *Bull. Soc. géol. Fr.* **6**, 965–971.

Bézert, P. & Caby, R. 1989. La déformation progressive de l'éocène de la région de Corte: nouvelle données pétrostructurales et conséquences pour la tectogénèse alpine en Corse. *C. r. hebd. séanc. Acad. Sci., Paris* 95–101.

Bird, P. 1991. Lateral extrusion of lower crust from under height topography in the isostatic limit. *J. geophys. Res.* **96**, 10275–10286.

Block, L. & Royden, L. 1990. Core complex geometries and regional scale flow in the lower crust. *Tectonics* **9**, 521–534.

Burrus, J. 1984. Contribution to a geodynamic synthesis of the Provençal basin (north-western Mediterranean). *Mar. Geol.* **55**, 247–269.

Carmignani, L. & Kligfield, R. 1990. Crustal extension in the northern Apennines: the transition from compression to extension in the Alpi Apuane core complex. *Tectonics* **9**, 1275–1305.

Caron, J. M. 1977. Lithostratigraphie et tectonique des schistes lustrés dans les Alpes cottiennes septentrionales et en Corse orientale. *Sci. géol. Mém.* **48**.

Caron, J. M., Kienast, J. R. & Triboulet, C. 1981. High pressure–low temperature metamorphism and polyphase Alpine deformation at Sant' Andrea di Cotone (Eastern Corsica, France). *Tectonophysics* **78**, 419–451.

Choukroune, P. & Lagarde, J. L. 1977. Plan de schistosité et déformation rotationelle: l'exemple du gneiss de Champtoceaux (Massif Armoricain). *C. r. hebd. Séanc. Acad. Sci., Paris* **284**, 2331–2334.

Cohen, C. R., Schweikert, R. A. & Odom, A. L. 1981. Age of emplacement of the Schistes Lustrés Nappe, Alpine Corsica. *Tectonophysics* **72**, 267–284.

Counas, D. 1986. Les unités alpines—autochtone et allochtone—à l'Ouest de Ghisonaccia (Corse Sud-Orientale). Thesis, University of Toulouse (Paul Sabatier).

Debrand-Passard, S. & Courbouleix, S. 1984. Synthèse géologique du Sud-Est de la France. *Mémoir. Bureau de la Recherche Géologique et Miniére* **126**.

Dewey, J. F., Helman, M. L., Torco, E., Hutton, D. H. W. & Knott, S. D. 1989. Kinematics of the Western Mediterranean. In: *Alpine Tectonics* (edited by Coward, M. P., Dietrich, D. & Park, R. G.). *Geol. Soc. Spec. Pub.* **45**, 265–283.

Durand Delga, M. 1984. Principaux trait de la Corse alpine et corrélation avec les Alpes ligures. *Mem. Soc. Geol. It.* **28**, 285–329.

Egal, E. 1989. Tectonique de l'Eocene en Corse. Thesis, University of Lyon (Claude Bernard—Lyon I, France).

Egal, E. 1992. Structures and tectonic evolution of the external zone of Alpine Corsica. *J. Struct. Geol.* **14**, 1215–1228.

Egal, E. & Caron, J. M. 1988. Tectonique polyphasée dans l'Eocène autochtone à la bordure ouest de la nappe de Balagne (Corse). *Bull. Soc. géol. Fr.* **2**, 315–321.

Essene, E. J. 1969. Relatively pure jadeite from a siliceous corsican gneiss. *Earth Planet. Sci. Lett.* **5**, 270–272.

Evans, B. W. 1990. Phase relations in epidote-blueschists. *Lithos* **25**, 3–23.

Faure, M. & Malavieille, J. 1981. Étude structurale d'un cisaillement ductile: le charriage ophiolitique Corse dans la région de Bastia. *Bull. Soc. géol. Fr.* **23**, 335–343.

Fournier, M., Jolivet, L., Goffé, B. & Dubois, R. 1991. The Alpine Corsica metamorphic core complex. *Tectonics* **10**, 1173–1186.

Gennesseaux, M., Réhault, J. P. & Thomas, B. 1989. La marge continentale de la Corse. *Bull. Soc. géol. Fr.* **5**, 339–351.

Ghosh, S. K. & Ramberg, H. 1976. Reorientation of inclusions by a combination of pure shear and simple shear. *Tectonophysics* **34**, 1470.

Gibbons, W. & Warburton, J. 1986. The blueschist facies schistes lustrés of Alpine Corsica: a review. *Geol. Soc. Am. Mem.* **164**, 301–311.

Gibbons, W. & Horak, J. 1984. Alpine metamorphism of Hercynian hornblende granodiorite beneath the blueschists facies Schistes Lustrés Nappe of NE Corsica. *J. metam. Geol.* **2**, 95–113.

Gillet, P. & Goffé, B. 1988. On the significance of aragonite occurrence in the Western Alps. *Contr. Miner. Petrol.* **99**, 70–81.

Goffé, B. & Velde, B. 1984. Contrasted metamorphic evolutions in the thrusted cover units of Briançonnais zone (French Alps): a model for the conservation of HP–LT metamorphic assemblages. *Earth Planet. Sci. Lett.* **68**, 351–360.

Goffé, B. & Vidal, O. 1992. Evidence for the controlling effect of high-pressure metamorphic *PTt* path on the mass transfer of major elements. In: *Water–Rocks Interaction* (edited by Kharaka, Y. K. & Maest, A. S.). Balkema, Rotterdam, 1499–1502.

Guillou, J. 1982. Etude géologique et métallogénique de la partie septentrionale du Cap Corse. Thesis, University of Paris.

Guiraud, M. 1982. Géothermomètrie du facies schistes verts à glaucophane, modellisation et applications (Afghanistan, Pakistan, Corse, Bohême). Thesis, University of Montpellier (France).

Harris, L. 1984. Déformations et déplacements dans la chaine alpine: l'exemple des schistes llustré du Cap Corse. Thesis, University of Rennes (France).

Hirn, A. & Sapin, M. 1976. La croute terrestre sous la Corse: données sismiques. *Bull. Soc. géol. Fr.* **18**, 1195–1199.

Jackson, M. D. & Ohnenstetter, M. 1981. Péridotite and gabbroic structures in the Monte Maggiore massif, alpine Corsica. *J. Geol.* **89**, 703–719.

Jolivet, L., Daniel, J. M. & Fournier, M. 1991. Geometry and kinematics of ductile extension in alpine Corsica. *Earth Planet. Sci. Lett.* **104**, 278–291.

Jolivet, L., Dubois, R., Fournier, M., Goffé, B., Michard, A. & Jourdan, C. 1990. Ductile extension in Alpine Corsica. *Geology* **18**, 1007–1010.

Jourdan, C. 1988. Balagne orientale et massif du Tende (Corse septentrionale). Etude structurale, interprétation des accidents et des déformations, reconstitutions géodynamiques. Thesis, University of Paris Sud, Orsay (France).

King, G., Ouyang, Z., Papadimitriou, P., Deschamps, A., Gagnepain, A., Houseman, G., Jackson, J., Soufleris, C. & Virieux, J. 1985. The evolution of the Gulf of Corinth (Greece) an aftershock study of the 1981 earthquake. *Geophys. J. R. astr. Soc.* **80**, 677–693.

Lahondère, D. 1988. Le métamorphisme éclogitique dans les orthogneiss et les métabasites ophiolitiques de la région de Farinole (Corse). *Bull. Soc. géol. Fr.* **4**, 579–586.

Lahondère, J. C. & Lahondère, D. 1988. Organisation structurale des schistes lustrés du Cap Corse. *C. r. hebd. Séanc. Acad. Sci., Paris* **307**, 1081–1086.

Mailhé, D. 1982. Application des méthodes de datation $^{39}Ar/^{40}Ar$ et traces de l'uranium à l'etude du déroulement de l'orogénèse alpine en Corse. Thesis, University of Montpellier (France).

Malavieille, J. 1982. Etude tectonique et microtectonique de la déformation ductile dans de grands chevauchements crustaux: exemple des Alpes franco-italiennes et de la Corse. Thesis, University of Montpellier (France).

Malavieille, J. 1983. Étude tectonique et microtectonique de la nappe de socle de Centuri (zone des schistes lustrés de Corse); conséquences pour la géométrie de la chaine alpine. *Bull. Soc. géol. Fr.* **7**, 195–204.

Maluski, H. 1977. Application de la méthode ^{40}Ar–^{39}Ar aux minéraux des roches cristallines perturbées par des évènements thermiques et tectoniques en Corse. Thesis, University of Montpellier (France).

Maluski, H., Mattauer, M. & Matte, P. 1973. Sur la présence de décrochements alpins en Corse. *C. r. hebd. Séanc. Acad. Sc., Paris* **276**, 709–712.

Mattauer, M., Faure, M. & Malavieille, J. 1981. Transverse lineation and large scale structures related to alpine obduction in Corsica. *J. Struct. Geol.* **3**, 401–409.

Miller, E. L., Gans, P. B. & Garling, J. 1983. The Snake river decollement: an exumed Mid-Tertiary brittle–ductile transition. *Tectonics* **2**, 239–263.

Morelli, C., Gieze, P., Carrozo, M. T., Colombi, B., Guerra, I., Hirn, A., Letz, A., Nicolich, R., Prodehl, C., Reicher, C., Rover, M., Sapin, M., Scarascia, S. & Wigger, P. 1977. Crustal and upper mantle structure of the Northern Apennines, the Ligurian Sea and Corsica, derived from seismic and gravimetric data. *Boll. Geof. Teor. Appl.* **75–76**, 199–260.

Morillon, A. C. & Sosson, M. 1993. New apatite fission-track dating on the Provençal Margin (Southeastern France): consequence on the thermal evolution of the Upper Oligocene rifting. *Terra Abstracts* **5**, 173.

Ohnenstetter, D., Ohnenstetter, M. & Rocci, G. 1976. Etude des métamorphismes successifs des cumulats ophiolitiques de Corse. *Bull. Soc. géol. Fr.* **18**, 115–134.

Pequignot, G. & Potdevin, J. L. 1984. Métamorphisme et tectonique dans les schistes lustrés à l'Est de Corte (Corse). Thesis, University of Lyon (Claude Bernard—Lyon I, France).

Peterlongo, J. M. 1968. Les ophiolites et le métamorphisme à glaucophane dans le massif de l'Inzecca et la région de Vezzani (Corse). *Bull. Bureau de la Recherche Géologique et Minière* **1**, 1–91.

Platt, J. P. 1986. Dynamics of orogenic wedges and the uplift of high-pressure metamorphic rocks. *Geol. Soc. Am. Bull.* **97**, 1037–1053.

Platt, J. P. & Vissers, R. L. M. 1980. Extensional structures in anisotropic rocks. *J. Struct. Geol.* **2**, 397–410.

Réhault, J. P., Boillot, G. & Mauffret, A. 1984. The Western Mediterranean Basin geological evolution. *Mar. Geol.* **5**, 5447–477.

Roberts, A. M. & Jackson, J. 1991. Active normal faulting in central

Greece: an overview. In: *The Geometry of Normal Fault* (edited by Roberts, A. M., Yielding, G. & Greeman, B.). *Geol. Soc. Spec. Pub.* **56**, 125–142.

Sartori, M., Mascle, G. & Amaudric du Chaffaut, S. 1987. A review of circum-Tyrrhenian regional geology (edited by Kastens, K., Mascle, J., Auroux, C. *et al.*). *Proc. Init. Repts ODP* **107**, 37–63.

Séranne, M. & Séguret, M. 1987. The Devonian basins of Western Norway: tectonics and kinematics of extending crust. In: *Continental Extensional Tectonics* (edited by Coward, M. P., Dewey, J. F. & Hanckock, P. L.). *Spec. Pub. geol. Soc. Lond.* **28**, 537–548.

Warburton, J. 1986. The ophiolite-bearing Schistes Lustrés Nappe in Alpine Corsica: a model for the emplacement of ophiolites that have suffered HP/LT metamorphism. *Geol. Soc. Am. Mem.* **164**, 313–331.

Waters, C. N. 1989. The metamorphic evolution of the schistes lustrés ophiolite, Cap Corse, Corsica. In: *Evolution of Metamorphic Belts* (edited by Daly, J. S., Cliff, R. A. & Yardley, B. W. D.). *Spec. Publ. geol. Soc. Lond.* **43**, 557–562.

Waters, C. N. 1990. The cenozoic tectonic evolution of Alpine Corsica. *J. geol. Soc. Lond.* **147**, 811–824.

Wdowinski, S. & Axen, J. 1992. Isostatic rebond due to tectonic denudation: a viscous flow model of a layered lithosphere. *Tectonics* **11**, 303–315.

Wernicke, B. P. & Axen, G. J. 1988. On the role of isostasy in the evolution of normal fault systems. *Geology* **16**, 848–851.

Zitellini, N., Trincardi, F., Marani, M. & Fabbri, A. 1986. Neogene tectonics of the Northern Tyrrhenian Sea. *G. Geol.* **48**(1–2), 25–40.